

## ORIGINAL ARTICLE

## Neuroprotective Effect of Shenfu Injection (参附注射液) Following Cardiac Arrest in Pig Correlates with Improved Mitochondrial Function and Cerebral Glucose Uptake\*

ZHANG Yi (张奕)<sup>1</sup>, LI Chun-sheng (李春盛)<sup>2</sup>, WU Cai-jun (吴彩军)<sup>2</sup>,  
YANG Jun (杨军)<sup>2</sup>, and HANG Chen-chen (杭晨晨)<sup>2</sup>

**ABSTRACT Objective:** To test whether Shenfu Injection (参附注射液, SFI) might attenuate the impact of cerebral energy dysfunction after resuscitation in a pig model of cardiac arrest (CA). **Methods:** Thirty-four Wuzhishan miniature inbred pigs were randomly divided into three groups: the SFI group ( $n=12$ ), the saline group (SA group,  $n=12$ ), and the sham-operated group (sham group,  $n=10$ ). Following successful return of spontaneous circulation (ROSC) from 8-min untreated ventricular fibrillation, animals received a continuous infusion of either SFI (0.2 mL/min) or saline for 6 h. Cerebral performance category score was evaluated at 24 and 48 h after ROSC, followed by positron emission tomography and computed tomography scans of cerebral glucose uptake. Surviving pigs were euthanized 48 h after ROSC, and the brains were removed for detecting mitochondrial function. **Results:** Compared with the SA group, SFI treatment produced a better neurologic outcome 48 h after ROSC ( $P<0.05$ ). However, there was no significant difference of survival rate between the SA and SFI groups (83.3% vs. 81.8%,  $P>0.05$ ). After ROSC, the SA group showed a decrease in the maximum standardized uptake value of different regions in the brain tissue, where SFI treatment can ameliorate these decreases ( $P<0.01$  or  $P<0.05$ ). Improved mitochondrial respiratory properties and higher mitochondrial membrane potential were also found following SFI treatment compared with the SA group at 48 h after ROSC ( $P<0.05$  or  $P<0.01$ ). **Conclusion:** SFI treatment after resuscitation has significant neuroprotective effects against disruption of cerebral energy metabolism from CA by improving glucose uptake and by normalizing mitochondrial function.

**KEYWORDS** cardiopulmonary resuscitation, Shenfu Injection, positron emission tomography/computed tomography, mitochondrial membrane potential, mitochondrial respiratory property, Chinese medicine

Cardiac arrest (CA) is the cessation of cardiac mechanical activity, which is confirmed by the absence of signs of circulation. Despite improvements in resuscitation techniques, out-of-hospital CA still results in poor outcomes.<sup>(1)</sup> Neurological injury remains a leading problem in patients following return of spontaneous circulation (ROSC), which is closely related to a high mortality and poor quality of life.<sup>(2,3)</sup>

Brain tissue is particularly susceptible to hypoxic-ischemic injury owing to features of energy metabolism, including high energy consumption, limited intrinsic energy stores, and a critical dependence on aerobic metabolism of glucose.<sup>(4,5)</sup> Mitochondria are crucial cellular organelles for energy production. Accumulating evidence shows that mitochondria play a critical role as effectors and targets of ischemia-reperfusion (IR) injury after CA.<sup>(6)</sup> Our previous study showed that hypothermia-induced neuroprotection was associated with reduced mitochondrial membrane permeability.<sup>(7)</sup>

Shenfu Injection (参附注射液, SFI) is an extract of Chinese herbs that has been reported to protect myocardial mitochondria injury during IR in rabbits.<sup>(8)</sup> The main active components of SFI are ginsenoside and higenamine. Ginsenosides are the most active ingredients in *Radix Ginseng* and have been classified as protopanaxadiol (PPD)-type or protopanaxatriol (PPT)-type.<sup>(9,10)</sup> In recent years, the PPT-type ginsenoside Rg1 and the PPD-type ginsenoside Rd have been reported as potentially neuroprotective agents.<sup>(11,12)</sup> Higenamine, on the other hand, has been

©The Chinese Journal of Integrated Traditional and Western Medicine Press and Springer-Verlag Berlin Heidelberg 2014

\*Supported by the Beijing Natural Science Foundation (No. 7132092) and Beijing Scientific Research Project for Outstanding Doctoral Thesis Guidance Teacher (No. 20121002501)

1. Department of Hyperbaric Oxygen, Beijing Chao-Yang Hospital, Capital Medical University, Beijing (100020), China; 2. Department of Emergency, Beijing Chao-Yang Hospital, Capital Medical University, Beijing (100020), China

Correspondence to: Dr. LI Chun-Sheng, Tel: 86-10-85231051, Fax: 86-10-85231051, E-mail: lcscyy@163.com

DOI: 10.1007/s11655-014-1890-7

reported to reduce apoptotic cell death in myocardial IR injury.<sup>(13)</sup> SFI is believed to be neuroprotective against IR injury, including blockade of Ca<sup>2+</sup> overload, suppression of inflammation, and prevention of neuronal apoptosis.<sup>(14,15)</sup> An allergic reaction to SFI is the most serious clinical adverse drug reaction, whereas other adverse effects are mild.<sup>(14)</sup> However, the effects of SFI on cerebral energy metabolism after CA, such as glucose uptake and mitochondrial respiration function, are relatively unknown.

Positron emission tomography (PET) with the glucose analogue <sup>18</sup>F-fluorodeoxyglucose (<sup>18</sup>F-FDG) is a non-invasive imaging technique for the *in vivo* quantitation and evaluation of regional cerebral glucose metabolism. Because glucose is the primary fuel source under normal conditions in the adult, PET with <sup>18</sup>F-FDG is considered to be the most reliable imaging modality,<sup>(16)</sup> and is potentially useful for investigating the changes following treatment interventions.<sup>(17)</sup> Combined PET and computed tomography (PET/CT) scanners allow precision of the anatomical location of glucose uptake.<sup>(18)</sup> Furthermore, PET has been used to detect residual brain tissue function in patients with post-anoxic encephalopathies due to CA.<sup>(19)</sup>

To test whether SFI given in the early post-resuscitation phase could attenuate cerebral energy metabolism dysfunction in a pig CA model, <sup>18</sup>F-FDG PET/CT imaging was employed to evaluate disruption of cerebral glucose uptake, while mitochondrial respiratory properties (MRPs) and mitochondrial membrane potential (MMP) were also assessed.

## METHODS

### Animal

Thirty-four healthy, male Wuzhishan miniature inbred pigs (animal license No. Beijing 2008-050109, provided by Chinese Academy of Agricultural Sciences) aged 3–4 months, with an average weight of 21 ± 3 kg were used in this study. All animals were under standard condition of temperature 25 ± 2 °C, relative humidity 60% ± 5% and 12 h-light/dark cycle. Prior to procedures, animals were fasted overnight except for free access to water. The experimental protocol was approved by the Animal Experimentation Ethics Committee of Capital Medical University, China (Permit No. 2010-D-013). Anesthesia was used in all surgical interventions to minimize animal suffering. All CA data were collected according to the Utstein

reporting guidelines updated in 2004.<sup>(20)</sup>

### Drugs and Reagents

SFI was purchased from Ya'an Sanjiu Pharmaceutical Co., Ltd., China, which is composed of *Panax Ginseng* C.A. Mey. and *Radix Aconitum Carmichaeli*. <sup>18</sup>F-FDG was from HTA Co., Ltd., Beijing, China. The mitochondrial isolation kit was from GENMED Scientific, USA. 5,5',6,6'-tetrachloro-1,1',3,3'-tetraethylbenzimidazol-carbocyanine iodide (JC-1) was from Sigma-Aldrich, St. Louis, MO, USA.

### Instruments

Servo 900C ventilator was from Siemens, Berlin, German. CO<sub>2</sub>SMOPlus monitor was from Respiration Inc., Murrysville, PA, USA. M1165 monitoring system was from Hewlett-Packard, Palo Alto, CA, USA. GY-600A electrical stimulator was from Kaifeng Huanan Equipment Co., Ltd., Henan, China. HeartStart MRx monitor/defibrillator was from Philips Medical Systems, Best, Holland. GEM Premier 3000 was from Instrumentation Laboratory, Lexington, MA, USA. The PET/CT scanner (GE Discovery STE) was from GE Healthcare, Waukesha, WI, USA. The Clark-type oxygen electrode using a Hansatech oxygraph measurement system was from Hansatech, Norfolk, UK. The transmission electron microscopy (H-7650) was from Hitachi, Ibaraki, Japan. The 7F Swan-Ganz catheter was from Edwards Life Sciences, Irvine, CA, USA.

### Animal Preparation

The pigs were randomly divided into three groups with the use of sealed envelopes: the SFI group (*n*=12), the saline group (SA group, *n*=12), and the sham-operated group (sham group, *n*=10). Following intramuscular administration of 10 mg/kg ketamine, pigs were anesthetized with ear vein injection of propofol (1 mg/kg). Surgical anesthesia was maintained with intravenous infusion of propofol 9 mg/(kg·h) and fentanyl 4 μg/(kg·h).

Animals were intubated with cuffed 6.5-mm endotracheal tubes and mechanically ventilated with a volume-controlled ventilator with a tidal volume of 8 mL/kg, at a respiratory rate of 12 breaths/min and an inspired oxygen fraction of 0.21. The end-tidal carbon dioxide pressure was monitored by a CO<sub>2</sub>SMOPlus monitor. Parameters of the ventilator were adjusted to maintain normocapnia (end-tidal PCO<sub>2</sub> of 35–40 mm Hg) before inducing CA.

A 5F pacing catheter was placed from the right femoral vein into the right ventricle. To induce ventricular fibrillation (VF), a 7F Swan-Ganz catheter was inserted from the right femoral vein to the pulmonary artery to measure right atrial pressure and cardiac output (CO). A fluid-filled catheter was advanced from the left femoral artery into the thoracic aorta to measure aortic pressure. M1165 monitoring system was used to monitor the electrocardiographic and hemodynamic parameters. Animals were allowed 30 min for hemodynamic stabilization prior to induction of VF.

### **Establishment of Programmed Electrical Stimulation-Induced CA Model**

In the SFI and SA groups, VF was induced by programmed electric stimulation as described by Wu, et al.<sup>(21)</sup> An electrical stimulator was set at the S1S2 protocol (300/200 ms), 40 V, 8:1 proportion and –10 ms step length until VF was achieved. VF was verified by electrocardiogram and blood pressure (whereby mean aortic pressure rapidly declined towards 0). Mechanical ventilation was ceased while inducing VF, and was withheld for the entire 8-min duration of VF-induced CA.

### **Cardiopulmonary Resuscitation and Advanced Life Support**

After 8-min untreated CA, mechanical ventilation was resumed with 100% oxygen, and cardiopulmonary resuscitation (CPR) was initiated manually at a frequency of 100 compressions per minute. The quality of chest compressions were controlled by a HeartStart MRx monitor/defibrillator with Q-CPR. The same CPR technicians were used to perform chest compressions in all animals. After 2-min CPR, pigs received a central venous injection of epinephrine (0.02 mg/kg). If VF persisted for another 2-min CPR, defibrillation was attempted once using a biphasic 3 J/kg stimulus (SMART Biphasic). If spontaneous circulation was still not achieved, CPR was continued for a further 2 min, and defibrillation was attempted once more (energy was increased in 1 J/kg increments).<sup>(22)</sup> The above sequence continued until ROSC was achieved. ROSC was defined as aortic systolic pressure greater than 50 mm Hg that was continuously sustained for at least 10 min. If ROSC was not achieved within 30 min, CPR was ceased and the animals were regarded as dead.

The successfully resuscitated pigs were treated with SFI (0.2 mL/min) or saline (0.2 mL/min), respectively. The drug injection began 15 min after ROSC and continued for

6 h by an infusion pump. The investigators were blinded to the drug treatments. Pigs in the sham group underwent anesthesia, surgery, mechanical respiration and 8-min withholding ventilation, without CA initiation or drugs. For replenishing fluid losses, 10 mL/(kg·h) normal saline was given intraoperatively to all animals.

All surviving animals underwent intensive care for 6 h, and mechanical ventilation was resumed. After the 6-h intensive care period all the catheters were removed. The animals were extubated after adequate inspiration depth was ascertained and the SpO<sub>2</sub> measurement was >97%.<sup>(23)</sup> The animals were allowed to recover from anesthesia, and were then placed in observation areas and monitored for a further 42 h. Both 23.5 and 47.5 h after ROSC, <sup>18</sup>F-FDG, the imaging tracer for the PET/CT scan, was injected into the vein.

### **Hemodynamic Measurement**

Heart rate (HR), mean arterial pressure (MAP) and CO were continuously monitored from baseline to 6 h after ROSC, and recorded at baseline, 1, 2, 4 and 6 h after ROSC.

### **Measurement of Arterial Blood Gas Analysis Parameters and Blood Glucose**

Arterial PO<sub>2</sub>, PCO<sub>2</sub>, pH and lactate were measured by arterial blood gas sampling using GEM Premier 3000 at baseline, 1, 2, 4, and 6 h after ROSC. Venous blood samples were taken for measurement of blood glucose at 24 and 48 h.

### **Neurological Evaluation**

To assess neurologic outcome, the cerebral performance category (CPC) score was evaluated by two investigators blinded to the treatment at both 24 and 48 h after ROSC. The CPC score ranges from 1 to 5 (1, intact function; 2, mild disability; 3, severe disability; 4, coma; and 5, brain death). Animals with a CPC score of 1 or 2 were classified as having a favorable outcome, while animals with a CPC score of 3–5 were classified as having an unfavorable outcome.<sup>(24)</sup>

### **Brain Glucose Metabolism by PET/CT**

To investigate brain glucose uptake, a PET/CT scanner was used. The <sup>18</sup>F-FDG (>95% purity coefficient generated) was injected into the vein at a dose of 5.55 mBq/kg approximately 45 min before imaging. After CPC evaluation at 24 h after ROSC, the animals were positioned prone on the scanning table following

intramuscular injection of ketamine (8 mg/kg) and an ear vein injection of propofol (1 mg/kg). The PET scan was performed following reconstruction of the CT images (3.75 mm section thickness at 3 mm intervals). Three-dimensional surface rendering technology was used to visualize the region of interest (ROI; diameter 0.3 cm). Two nuclear medicine physicians, blinded to the treatment, measured the maximum standardized uptake value ( $SUV_{max}$ ) of the parietal lobe, frontal lobe, brain stem and cerebellum. The PET/CT scan was repeated after CPC evaluation at 48 h after ROSC.

### Detection of Mitochondrial Function

Upon completion of the PET/CT scan at 48 h after ROSC, surviving animals were euthanized with 20 mL potassium chloride (10 mol/L) intravenously. The brain was immediately removed by craniotomy and divided midsagittally. Frontal cortex samples were collected on ice and stored at  $-80^{\circ}\text{C}$  until isolation of mitochondria. Mitochondria from brain tissues were isolated with a mitochondrial isolation kit following the manufacturer's instructions. The key steps are as follows: brain tissues were washed in ice-cold buffer, cut into small pieces using scissors and homogenized using a glass homogenizer. Thereafter, the homogenate was added to ice-cold isolation medium and centrifuged at  $1,500 \times g$  at  $4^{\circ}\text{C}$  for 10 min. The supernatant was centrifuged again at  $10,000 \times g$  at  $4^{\circ}\text{C}$  for 10 min. Finally, the resulting pellet was added to ice-cold preservation solution and centrifuged at  $10,000 \times g$  at  $4^{\circ}\text{C}$  for 5 min. The protein concentration of the isolated mitochondria was determined by the Bradford method<sup>(7)</sup> and kept on ice for further experimental assays.

### MRPs

A Clark-type oxygen electrode using a hansatech oxygraph measurement system was used to measure oxygen uptake. State 3 respiration and state 4 respiration were monitored as described by Gong, et al.<sup>(7)</sup> The definition of respiratory control ratio (RCR) was state 3 respiration divided by state 4 respiration, while the definition of adenosine diphosphate (ADP)/O ratio was moles of ADP phosphorylated per moles of oxygen consumed.

### Detection of MMP

MMP was monitored as described by Gong, et al.<sup>(7)</sup> Briefly, mitochondria (40 mg) were added to 2 mL incubation buffer. The reaction was initiated by addition of JC-1 to a final concentration of 10 mg/mL, and the

mitochondria were then left to incubate for 7 min at room temperature in the dark. A spectrofluorimeter (Infinite M200; Tecan, CH) was used to analyze the fluorescence of the sample. The excitation wavelength was 490 nm, while the emission wavelength was 590 nm.

### Brain Ultramicrostructure

For morphologic examination, another portion of the frontal cortex was collected on ice and preserved in 10% formaldehyde and 4% paraformaldehyde. The ultramicrostructure of brain tissue was observed using a transmission electron microscopy.

### Statistical Analysis

Statistical analysis was performed with SPSS 17.0 software (SPSS, Chicago, IL, USA). Continuous variables were presented as mean  $\pm$  standard deviation ( $\bar{x} \pm s$ ). One-way repeated-measures analysis of variance (ANOVA) was used to determine differences over time within groups. Comparisons between groups were made with a one-way ANOVA, and Bonferroni's test was used for post hoc comparisons. The Fisher's exact test was used to compare discrete variables.  $P < 0.05$  was considered statistically significant.

## RESULTS

### Resuscitation Outcome, Survival Rate and Neurologic Outcome

Twenty-three of 24 animals were successfully resuscitated in the two resuscitation groups (12 in the SA group, and 11 in the SFI group). By comparison, ROSC rate (100.0% vs. 91.7%) and CPR time (min,  $4.8 \pm 1.2$  vs.  $5.0 \pm 1.5$ ) did not differ significantly between the SA and SFI groups ( $P > 0.05$ ). Ten pigs in the SA group, 9 in the SFI group, and 10 in the sham group survived to 48 h. There were no significant differences in 24- and 48-h survival rates between SA and SFI groups ( $P > 0.05$ ). More animals in the SFI group were classified as having a favorable outcome than those in the SA group at 48 h after ROSC ( $P = 0.035$ ), but there were no significant differences in the 24-h favorable outcome rates between the SA and SFI groups ( $P > 0.05$ , Table 1).

### Comparisons of Hemodynamic Parameters

HR, MAP and CO at baseline did not differ significantly among the three groups ( $P > 0.05$ ). In the SA and SFI groups, HR was significantly increased and CO was significantly decreased at 1–6 h after ROSC compared with baseline and the sham group at the same time ( $P < 0.01$  or  $P < 0.05$ ). MAP in the



**Table 1. Comparisons of Survival Rate and Neurologic Outcome between the SA and SFI Groups [n (%)]**

Group	n	Survival		Favorable outcome	
		24 h	48 h	24 h	48 h
SA	12	10 (83.3)	10 (83.3)	2 (16.7)	4 (33.3)
SFI	11	9 (81.8)	9 (81.8)	4 (36.4)	9 (81.8)*

Note: \*P<0.05, compared with the SA group at the same time

SA group was significantly increased at 1 h and decreased at 4 h after ROSC, while in the SFI group, it was significantly increased at 1 and 2 h after ROSC (P<0.01). By contrast, there were no significant differences in HR at any time after ROSC between the SA and SFI groups (P>0.05). MAP and CO were significantly higher in the SFI group than in the SA group at 1–6 h after ROSC (P<0.01 or P<0.05, Figure 1).

**Comparison of Arterial Blood Gases and Lactate Level**

Arterial PO<sub>2</sub>, PCO<sub>2</sub>, pH, and lactate levels at baseline did not differ significantly among the three groups (P>0.05). In the SA and SFI groups, the pH was significantly decreased at 1, 2, 4 h after ROSC compared with baseline and the sham group at the same time, whereas PO<sub>2</sub> at 1, 2 h after ROSC, PCO<sub>2</sub> at 1 h after ROSC and lactate at 1, 2, 4 h after ROSC were significantly increased (P<0.01 or P<0.05). By comparison, pH was higher in the SFI group than in the SA group at 1 and 2 h after ROSC, while lactate was lower (P<0.05). There were no significant

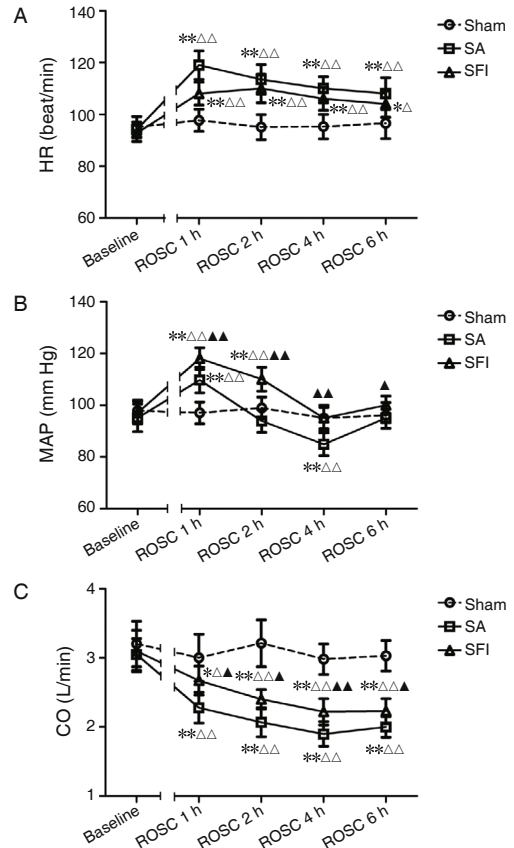


**Figure 1. Comparisons of Hemodynamic Parameters ( $\bar{x} \pm s$ )**

Notes: \*P<0.05, \*\*P<0.01, compared with the baseline values; ΔP<0.05, ΔΔP<0.01, compared with the sham group at the same time; ▲P<0.05, ▲▲P<0.01, compared with the SA group at the same time

differences in PO<sub>2</sub> and PCO<sub>2</sub> at any time after ROSC between the SA and SFI groups (P>0.05, Figure 2).

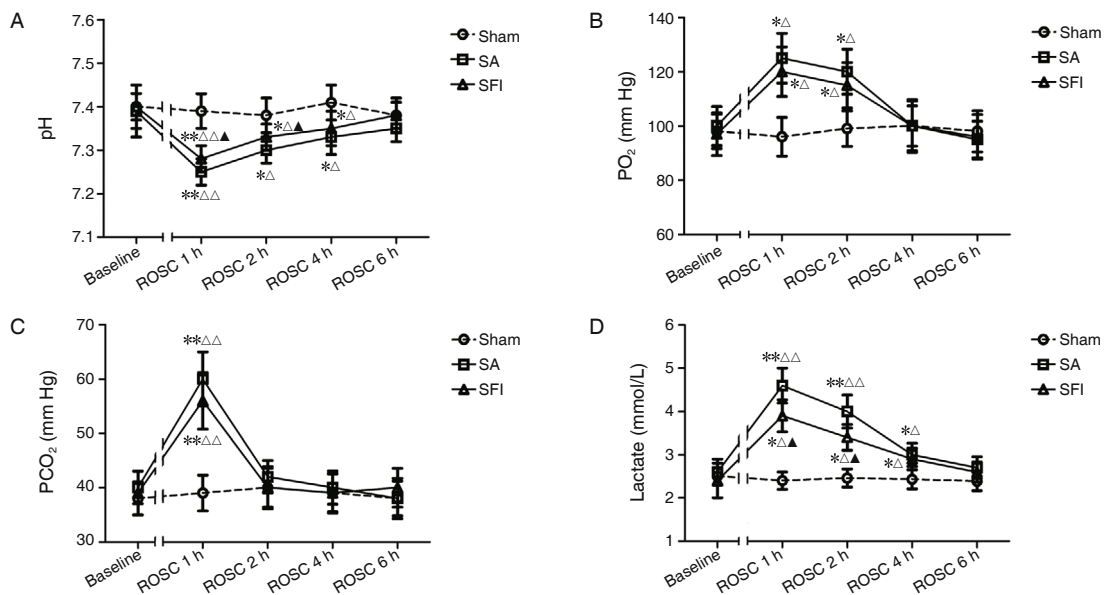


**Figure 2. Comparisons of Arterial Blood Gases and Lactate Level ( $\bar{x} \pm s$ )**

Notes: \*P<0.05, \*\*P<0.01, compared with the baseline values; ΔP<0.05, ΔΔP<0.01, compared with the sham group at the same time; ▲P<0.05, compared with the SA group at the same time

**Glucose Metabolism of Brain Tissue**

The dosages of propofol and levels of blood glucose among three groups did not differ before PET/CT scans ( $P>0.05$ , Table 2). Figure 3 shows the images of PET/CT scan after 24 and 48 h of ROCS. After 24 h of ROCS, resuscitation groups showed a decrease in the  $SUV_{max}$  of the parietal lobe, frontal lobe, brain stem and cerebellum compared with the sham group ( $P<0.01$ ). Compared with the SA group, the  $SUV_{max}$  of different regions in the SFI group was significantly increased ( $P<0.01$  or  $P<0.05$ ). After 48 h of ROCS, the  $SUV_{max}$  of the cerebellum and brain stem did not differ among the three groups ( $P>0.05$ ). However, the  $SUV_{max}$  of the parietal lobe and frontal lobe in the SA group were significantly lower than those in the sham group ( $P<0.01$ ), and SFI treatment alleviated these decreases ( $P<0.05$ , Figure 4).

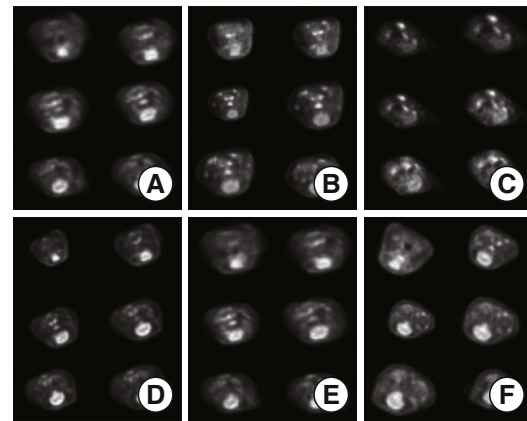


**Figure 3. Images of PET/CT Scan 24 and 48 h after ROCS**

Notes: A: sham group 24 h after ROCS; B: SFI group 24 h after ROCS; C: SA group 24 h after ROCS; D: sham group 48 h after ROCS; E: SFI group 48 h after ROCS; F: SA group 48 h after ROCS

**Table 2. Comparisons of Propofol Dosage and Blood Glucose before PET/CT Scan ( $\bar{x} \pm s$ )**

Group	n	Propofol dosage (mg)		Blood glucose (mmol/L)	
		24 h	48 h	24 h	48 h
Sham	10	23.1 ± 2.1	25.2 ± 2.3	7.9 ± 0.5	7.4 ± 0.5
SA	10	25.2 ± 2.5	23.4 ± 2.5	8.5 ± 0.6	8.1 ± 0.7
SFI	9	24.9 ± 2.3	24.7 ± 2.2	8.2 ± 0.6	7.9 ± 0.5

**MRPs and MMP**

As shown in Table 3, after 48 h of ROCS, animals in the SA and SFI groups exhibited lower values of state 3 respiration, RCR, ADP/O ratios and MMP, and higher values of state 4 respiration compared with those in the sham group ( $P<0.01$ ). Compared with the SA group, animals in the SFI group showed a higher state 3 respiration, RCR, ADP/O ratio and MMP, and a lower state 4 respiration ( $P<0.01$  or  $P<0.05$ ).

**Brain Ultramicrostructure**

The SA group showed obvious nerve cell damage, including loss of normal nerve cell form, presence of nuclear deformation and solid shrinkage, mitochondrial swelling, ridge fracture, and cavity

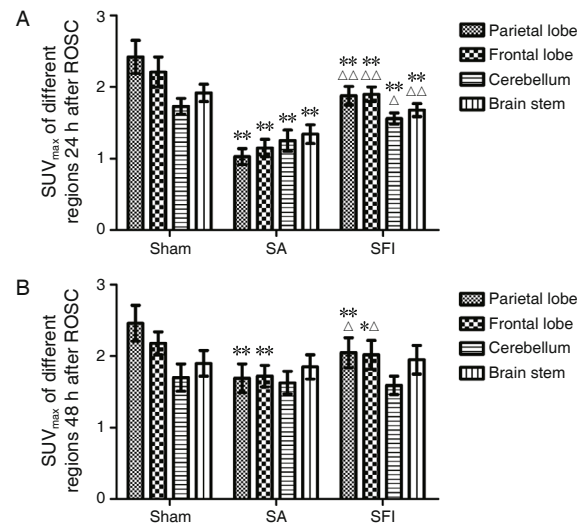


**Figure 4. Comparison of Glucose Uptake by Brain Tissue 24 and 48 h after ROCS ( $\bar{x} \pm s$ )**

Notes: \* $P<0.05$ , \*\* $P<0.01$ , compared with the sham group;  $\Delta P<0.05$ ,  $\Delta\Delta P<0.01$ , compared with the SA group

changes. Animals treated with SFI exhibited little intracellular damage in the mitochondrial architecture 48 h after ROCS (Figure 5).

**DISCUSSION**

In the present study, we found that SFI given in

**Table 3. Comparisons of MRPs and MMP 48 h after ROCS ( $\bar{x} \pm s$ )**

Group	n	MRPs				MMP (percentage of sham)
		State 3 respiration (nmol $O_2$ /min/mg protein)	State 4 respiration (nmol $O_2$ /min/mg protein)	RCR	ADP/O ratio	
Sham	10	110.5 ± 9.3	21.8 ± 1.9	5.1 ± 0.7	1.9 ± 0.1	98.3 ± 1.6
SA	10	66.5 ± 4.0*	30.8 ± 1.8*	2.1 ± 0.1*	1.1 ± 0.7*	64.1 ± 2.9*
SFI	9	88.7 ± 5.4* $\Delta\Delta$	25.1 ± 2.0* $\Delta\Delta$	3.5 ± 0.2* $\Delta\Delta$	1.5 ± 0.1* $\Delta\Delta$	70.0 ± 6.2* $\Delta$

Notes: \* $P<0.01$ , compared with the sham group;  $\Delta P<0.05$ ,  $\Delta\Delta P<0.01$ , compared with the SA group

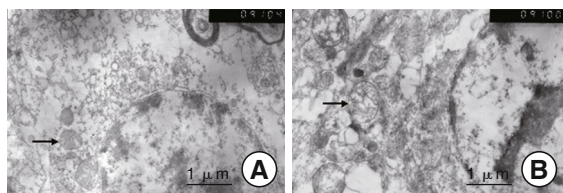


**Figure 5. Brain Ultramicrostructure of the Frontal Cortex Tissue by Electron Microscopy ( $\times 10,000$ )**

Notes: Arrows: mitochondria. A: the SFI group; B: the SA group

the early post-resuscitation phase attenuated brain injury and improved neurological outcome at 48 h after ROSC. Second, SFI improved cerebral glucose uptake when measured by PET/CT imaging. Third, SFI reduced brain mitochondrial dysfunction, as verified by MRPs and MMP. This evidence indicates that the neuroprotective effects of SFI on brain injury caused by CA might be associated with the improving cerebral energy metabolism.

CA results in whole-body IR injury, and CPR can only partially reverse this process.<sup>(25)</sup> Further, post-resuscitation cerebral injury as a result of brain IR occurs within hours to days after ROSC.<sup>(26)</sup> A lack of neuroprotective medications during the post-resuscitation period is one of the reasons for poor outcomes of CA. In our previous study, a continuous infusion of SFI for 6 h after ROSC was shown to attenuate post-resuscitation myocardial dysfunction in a 4-min untreated VF model.<sup>(27)</sup> In the present experiment, an 8-min untreated VF model was adopted to study the effect of SFI given in the early post-resuscitation phase on post-resuscitation cerebral dysfunction.

Glucose is the major energy substrate for mammalian brain metabolism. Therefore, the level of glucose utilization correlates with the degree of neuronal activity, and continuous glucose is required for proper neuronal function.<sup>(28)</sup> So, to test the effect of SFI on brain injury after CA, an  $^{18}\text{F}$ -FDG PET/CT scan was employed to investigate the brain glucose uptake using the semi-quantitative SUV. A reduction in glucose uptake measured by  $^{18}\text{F}$ -FDG PET has been reported in CA patients following 72 h of therapeutic hypothermia.<sup>(29)</sup> After 24 h post-resuscitation here, we observed reductions of  $\text{SUV}_{\text{max}}$  in the different brain regions, indicating that glucose metabolism was decreased significantly. Our results are consistent with the study of Schaafsma, et al,<sup>(30)</sup> in which the decreased cerebral glucose metabolism in CA patients at 24 h after ROSC was verified. In the SFI group here,  $^{18}\text{F}$ -FDG uptake was significantly increased compared with the SA group, showing that SFI can

improve glucose uptake after CA. At 48 h after ROSC, the glucose uptake of the parietal lobe and the frontal lobe in the SA group was still lower than that in the sham group; glucose uptake in the cerebellum and brain stem did not differ among the three groups. These results indicated that post-resuscitation cerebral dysfunction in the cerebral cortex was more severe than in the cerebellum and brain stem. Ginsenoside Rb1 has been reported to stimulate glucose uptake in adipocytes through an insulin-like signaling pathway.<sup>(31)</sup> Apart from this mechanism, how the active components of SFI affect the glucose uptake in the brain tissue is still unknown.

Mitochondria are the center of energy metabolism, and neurons critically depend on mitochondrial function to establish membrane excitability and to execute the complex processes of neurotransmission and plasticity.<sup>(32)</sup> Within 5 min of sudden CA, cerebral adenosine triphosphate (ATP) stores are exhausted.<sup>(33)</sup> In the early stage of post-ROSC, mitochondrial oxidative phosphorylation slows down, resulting in a reduced generation of ATP.<sup>(34)</sup> The formation of the MMP across the inner mitochondrial membrane drives the conversion of ADP to ATP via a series of respiratory chain enzymes, and differences in the extent of the MMP reflect variations in the mitochondrial activity and function.<sup>(35,36)</sup> Studies have shown that ginsenoside Rg3 has the effects in improving mitochondrial energy metabolism in the brain of rats.<sup>(37)</sup> Ginsenoside Rd has been reported to stabilize the MMP and attenuate the apoptotic death of hippocampal neurons after oxygen-glucose deprivation.<sup>(38)</sup> In this study, compared with the sham group, the cerebral cortex MRPs (including RCR and ADP/O) and MMP in the resuscitation groups decreased at 48 h after ROSC; these decreases were improved in the SFI group compared with the SA group. These results indicate that SFI treatment can improve cerebral MRPs and stabilize MMP after cardiac resuscitation.

Lower lactate, but higher pH, MAP and CO were also found in the SFI group, indicating that SFI treatment can attenuate myocardial dysfunction and acidosis. The 2010 American Heart Association Guidelines for Post-Cardiac Arrest Care recommend immediate treatment of hypotension to maintain adequate tissue perfusion,<sup>(39)</sup> higher MAP was associated with better outcomes in comatose survivors of CA patients.<sup>(40)</sup> Acidosis has been reported to correlate with greater cerebral ischemic-anoxic damage.<sup>(41)</sup> Thus, the benefit effects of SFI on

myocardial dysfunction and acidosis may partly explain the better neurologic outcome.

Some limitations of this study should be noted. This study was performed on healthy animals, whereas most CA patients have underlying diseases. Furthermore, we only evaluated the outcomes at 24 and 48 h after ROSC, a further study looking at 72 h or longer might help refine the evidence.

In conclusion, SFI might attenuate the post-resuscitation neurological dysfunction by improving glucose uptake and by normalizing mitochondrial function.

### Conflict of Interest

The authors declare that there is no conflict of interest regarding the publication of this paper.

### Author Contributions

Li CS contributed to the study design. Zhang Y, Wu CJ, and Yang J performed the data collection. Hang CC analyzed the data. Zhang Y drafted the manuscript. All authors read and approved the final version of the manuscript for publication.

### Acknowledgments

The authors thank the following persons for their technical assistance: GUO Zhi-jun, WANG Shuo, and YIN Qin (Department of Emergency, Beijing Chao-Yang Hospital, Capital Medical University), GONG Ping (Department of Emergence, The First Affiliated Hospital of Dalian Medical University), HOU Xiao-min (Department of Hyperbaric Oxygen, Beijing Chao-Yang Hospital, Capital Medical University), and WANG Tie, QU Shi-ying, and LIU Chang (Department of Nuclear Medicine, Beijing Chao-Yang Hospital, Capital Medical University).

## REFERENCES

- Iwami T, Nichol G, Hiraide A, Hayashi Y, Nishiuchi T, Kajino K, et al. Continuous improvements in "chain of survival" increased survival after out-of-hospital cardiac arrests: a large-scale population-based study. *Circulation* 2009;119:728-734.
- Busl KM, Greer DM. Hypoxic-ischemic brain injury: pathophysiology, neuropathology and mechanisms. *NeuroRehabilitation* 2010;26:5-13.
- Laver S, Farrow C, Turner D, Nolan J. Mode of death after admission to an intensive care unit following cardiac arrest. *Intensive Care Med* 2004;30:2126-2128.
- Jiang J, Fang X, Fu Y, Xu W, Jiang L, Huang Z. Impaired cerebral mitochondrial oxidative phosphorylation function in a rat model of ventricular fibrillation and cardiopulmonary resuscitation. *Biomed Res Int* 2014;2014:192769.
- Sharma AB, Barlow MA, Yang SH, Simpkins JW, Mallet RT. Pyruvate enhances neurological recovery following cardiopulmonary arrest and resuscitation. *Resuscitation* 2008;76:108-119.
- Gazmuri RJ, Radhakrishnan J. Protecting mitochondrial bioenergetic function during resuscitation from cardiac arrest. *Crit Care Clin* 2012;28:245-270.
- Gong P, Hua R, Zhang Y, Zhao H, Tang Z, Mei X, et al. Hypothermia-induced neuroprotection is associated with reduced mitochondrial membrane permeability in a swine model of cardiac arrest. *J Cereb Blood Flow Metab* 2013;33:928-934.
- Cao J, Zheng CD, Zhang GX, Zhang YJ, Min S. Protective effect of Shenfu Injection on myocardial mitochondria injured by ischemia-reperfusion in rabbits. *Chin Med J* 2005;118:505-507.
- Lu JM, Yao Q, Chen C. Ginseng compounds: an update on their molecular mechanisms and medical applications. *Curr Vasc Pharmacol* 2009;7:293-302.
- Leung KW, Wong AS. Pharmacology of ginsenosides: a literature review. *Chin Med J* 2010;5:20-24.
- Nah SY, Kim DH, Rhim H. Ginsenosides: are any of them candidates for drugs acting on the central nervous system? *CNS Drug Rev* 2007;13:381-340.
- Ye R, Li N, Han J, Kong X, Cao R, Rao Z, et al. Neuroprotective effects of ginsenoside Rd against oxygen-glucose deprivation in cultured hippocampal neurons. *Neurosci Res* 2009;64:306-310.
- Lee YS, Kang YJ, Kim HJ, Park MK, Seo HG, Lee JH, et al. Higenamine reduces apoptotic cell death by induction of heme oxygenase-1 in rat myocardial ischemia-reperfusion injury. *Apoptosis* 2006;11:1091-1100.
- Hou X, Li C, Gu W, Guo Z, Yin W, Zhang D. Effect of Shenfu on inflammatory cytokine release and brain edema after prolonged cardiac arrest in the swine. *Am J Emerg Med* 2013;31:1159-1164.
- Yang LJ, Wang J, Tian ZF, Yuan YF. Shenfu Injection attenuates neonatal hypoxic-ischemic brain damage in rat. *Neurol Sci* 2013;34:1571-1574.
- Li J, Gu L, Feng DF, Ding F, Zhu GG, Rong JD. Exploring temporospatial changes in glucose metabolic disorder, learning, and memory dysfunction in a rat model of diffuse axonal injury. *J Neurotrauma* 2012;29:2635-2646.
- Lou M, Zhang H, Wang J, Wen SQ, Tang ZQ, Chen YZ, et al. Hyperbaric oxygen treatment attenuated the decrease in regional glucose metabolism of rats subjected to focal cerebral ischemia: a high resolution positron emission tomography study. *Neuroscience* 2007;11:555-561.
- Eil PJ, von Schulthess GK. PET/CT: a new road map. *Eur J Nucl Med Mol Imaging* 2002;29:719-720.
- De Volder AG, Michel C, Guérit JM, Bol A, Georges B, de Barse T. Brain glucose metabolism in postanoxic syndrome due to cardiac arrest. *Acta Neurol Belg* 1994;94:183-189.



20. Neumar RW, Nolan JP, Adrie C, Aibiki M, Berg RA, Böttiger BW, et al. Post-cardiac arrest syndrome: epidemiology, pathophysiology, treatment, and prognostication: a consensus statement from the International Liaison Committee on Resuscitation (American Heart Association, Australian and New Zealand Council on Resuscitation, European Resuscitation Council, Heart and Stroke Foundation of Canada, InterAmerican Heart Foundation, Resuscitation Council of Asia, and the Resuscitation Council of Southern Africa); the American Heart Association Emergency Cardiovascular Care Committee; the Council on Cardiovascular Surgery and Anesthesia; the Council on Cardiopulmonary, Perioperative, and Critical Care; the Council on Clinical Cardiology; and the Stroke Council. *Circulation* 2008;118:2452-2483.
21. Wu JY, Li CS, Liu ZX, Wu CJ, Zhang GC. A comparison of 2 types of chest compressions in a porcine model of cardiac arrest. *Am J Emerg Med* 2009;27:823-829.
22. Killingsworth CR, Wei CC, Dell'Italia LJ, Ardell JL, Kingsley MA, Smith WM, et al. Short-acting beta-adrenergic antagonist esmolol given at reperfusion improves survival after prolonged ventricular fibrillation. *Circulation* 2004;109:2469-2474.
23. Pantazopoulos IN, Xanthos TT, Vlachos I, Troupis G, Kotsiomitis E, Johnson E, et al. Use of the impedance threshold device improves survival rate and neurological outcome in a swine model of asphyxial cardiac arrest. *Crit Care Med* 2012;40:861-868.
24. Ajam K, Gold LS, Beck SS, Damon S, Phelps R, Rea TD. Reliability of the cerebral performance category to classify neurological status among survivors of ventricular fibrillation arrest: a cohort study. *Scand J Trauma Resusc Emerg Med* 2011;19:38.
25. Herlitz J, Engdahl J, Svensson L, Angquist KA, Silfverstolpe J, Holmberg S. Major differences in 1-month survival between hospitals in Sweden among initial survivors of out-of-hospital cardiac arrest. *Resuscitation* 2006;70:404-409.
26. Noppens RR, Kelm RF, Lindemann R, Engelhard K, Werner C, Kempfski O. Effects of a single-dose hypertonic saline hydroxyethyl starch on cerebral blood flow, long-term outcome, neurogenesis, and neuronal survival after cardiac arrest and cardiopulmonary resuscitation in rats. *Crit Care Med* 2012;40:2149-2156.
27. Ji XF, Yang L, Zhang MY, Li CS, Wang S, Cong LH. Shen-fu Injection attenuates postresuscitation myocardial dysfunction in a porcine model of cardiac arrest. *Shock* 2013;35:530-536.
28. Kawai N, Maeda Y, Kudomi N, Yamamoto Y, Nishiyama Y, Tamiya T. Focal neuronal damage in patients with neuropsychological impairment after diffuse traumatic brain injury: evaluation using <sup>11</sup>C-flumazenil positron emission tomography with statistical image analysis. *J Neurotrauma* 2010;27:2131-2138.
29. Nakamura T, Kuroda Y, Torigoe N, Abe Y, Yamashita S, Kawakita K, et al. Cerebral metabolism monitoring during hypothermia following resuscitation from cardiopulmonary arrest. *Acta Neurochir Suppl* 2008;102:203-206.
30. Schaafsma A, de Jong BM, Bams JL, Haaxma-Reiche H, Pruijm J, Zijlstra JG. Cerebral perfusion and metabolism in resuscitated patients with severe post-hypoxic encephalopathy. *J Neurol Sci* 2003;210:23-30.
31. Shang W, Yang Y, Zhou L, Jiang B, Jin H, Chen M. Ginsenoside Rb1 stimulates glucose uptake through insulin-like signaling pathway in 3T3-L1 adipocytes. *J Endocrinol* 2008;198:561-569.
32. Kann O, Kovács R. Mitochondria and neuronal activity. *Am J Physiol Cell Physiol* 2007;292:C641-C657.
33. Safar P, Behringer W, Böttiger BW, Sterz F. Cerebral resuscitation potentials for cardiac arrest. *Crit Care Med* 2002;30(Suppl):S140-S144.
34. Weber J, Senior AE. ATP synthesis driven by proton transport in F1F0-ATP synthase. *FEBS Lett* 2003;545:61-70.
35. Mitchell M, Schulz SL, Armstrong DT, Lane M. Metabolic and mitochondrial dysfunction in early mouse embryos following maternal dietary protein intervention. *Biol Reprod* 2009;80:622-630.
36. Acton BM, Jurisicova A, Jurisica I, Casper RF. Alterations in mitochondrial membrane potential during preimplantation stages of mouse and human embryo development. *Mol Hum Reprod* 2004;10:23-32.
37. Tian J, Zhang S, Li G, Liu Z, Xu B. 20(S)-ginsenoside Rg3, a neuroprotective agent, inhibits mitochondrial permeability transition pores in rat brain. *Phytother Res* 2009;23:486-491.
38. Ye R, Li N, Han J, Kong X, Cao R, Rao Z, et al. Neuroprotective effects of ginsenoside Rd against oxygen-glucose deprivation in cultured hippocampal neurons. *Neurosci Res* 2009;64:306-310.
39. Peberdy MA, Callaway CW, Neumar RW, Geocadin RG, Zimmerman JL, Donnino M, et al. Part 9: post-cardiac arrest care: 2010 American Heart Association Guidelines for cardiopulmonary resuscitation and emergency cardiovascular care. *Circulation* 2010;122(Suppl):S768-S786.
40. Beylin ME, Perman SM, Abella BS, Leary M, Shofer FS, Grossestreuer AV, et al. Higher mean arterial pressure with or without vasoactive agents is associated with increased survival and better neurological outcomes in comatose survivors of cardiac arrest. *Intensive Care Med* 2013;39:1981-1988.
41. Isaev NK, Stelmashook EV, Plotnikov EY, Khryapenkova TG, Lozier ER, Doludin YV, et al. Role of acidosis, NMDA receptors, and acid-sensitive ion channel 1a (ASIC1a) in neuronal death induced by ischemia. *Biochemistry (Mosc)* 2008;73:1171-1175.

(Received July 3, 2014)  
 Edited by YU Ming-zhu